



Quantitative diffusion-weighted MRI response assessment in rhabdomyosarcoma: an international retrospective study on behalf of the European *paediatric* Soft tissue sarcoma Study Group Imaging Committee

Roelof van Ewijk¹ · Cyrano Chatziantoniou^{1,2} · Madeleine Adams³ · Patrizia Bertolini⁴ · Gianni Bisogno^{5,6} · Amine Bouhamama⁷ · Pablo Caro-Dominguez⁸ · Valerie Charon⁹ · Ana Coma¹⁰ · Rana Dandis¹ · Christine Devalck¹¹ · Giulia De Donno² · Andrea Ferrari¹² · Marta Fiocco^{1,13} · Soledad Gallego¹⁴ · Chiara Giraud¹⁵ · Heidi Glosli¹⁶ · Simone A. J. ter Horst¹⁷ · Meriel Jenney¹⁸ · Willemijn M. Klein¹⁹ · Alexander Leemans² · Julie Leseur²⁰ · Henry C. Mandeville²¹ · Kieran McHugh²² · Johannes H. M. Merks^{1,23} · Veronique Minard-Colin²⁴ · Salma Moalla²⁵ · Carlo Morosi²⁶ · Daniel Orbach²⁷ · Lil-Sofie Ording Muller²⁸ · Erika Pace²⁹ · Pier Luigi Di Paolo³⁰ · Katia Perruccio³¹ · Lucia Quaglietta³² · Marleen Renard³³ · Rick R. van Rijn³⁴ · Antonio Ruggiero³⁵ · Sara I. Sirvent³⁶ · Alberto De Luca^{2,37} · Reineke A. Schoot¹

Received: 5 June 2023 / Revised: 4 August 2023 / Accepted: 7 August 2023 / Published online: 8 September 2023
© The Author(s) 2023

Abstract

Objective To investigate the feasibility of diffusion-weighted magnetic resonance imaging (DW-MRI) as a predictive imaging marker after neoadjuvant chemotherapy in patients with rhabdomyosarcoma.

Material and methods We performed a multicenter retrospective study including pediatric, adolescent and young adult patients with rhabdomyosarcoma, Intergroup Rhabdomyosarcoma Study group III/IV, treated according to the European *paediatric* Soft tissue sarcoma Study Group (*EpSSG*) RMS2005 or MTS2008 studies. DW-MRI was performed according to institutional protocols. We performed two-dimensional single-slice tumor delineation. Areas of necrosis or hemorrhage were delineated to be excluded in the primary analysis. Mean, median and 5th and 95th apparent diffusion coefficient (ADC) were extracted.

Results Of 134 included patients, 82 had measurable tumor at diagnosis and response and DW-MRI scans of adequate quality and were included in the analysis. Technical heterogeneity in scan acquisition protocols and scanners was observed. Mean ADC at diagnosis was 1.1 (95% confidence interval [CI]: 1.1–1.2) (all ADC expressed in $\times 10^{-3}$ mm²/s), versus 1.6 (1.5–1.6) at response assessment. The 5th percentile ADC was 0.8 (0.7–0.9) at diagnosis and 1.1 (1.0–1.2) at response. Absolute change in mean ADC after neoadjuvant chemotherapy was 0.4 (0.3–0.5). Exploratory analyses for association between ADC and clinical parameters showed a significant difference in mean ADC at diagnosis for alveolar versus embryonal histology. Landmark analysis at nine weeks after the date of diagnosis showed no significant association (hazard ratio 1.3 [0.6–3.2]) between the mean ADC change and event-free survival.

Conclusion A significant change in the 5th percentile and the mean ADC after chemotherapy was observed. Strong heterogeneity was identified in DW-MRI acquisition protocols between centers and in individual patients.

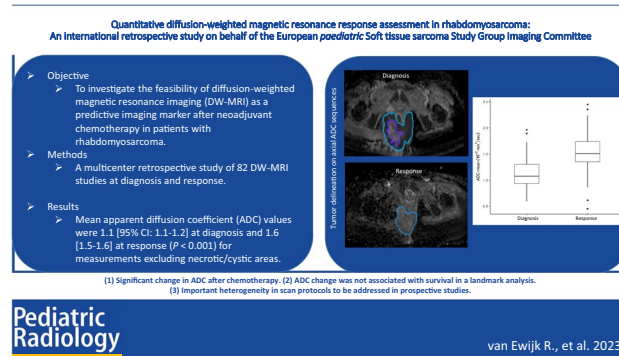
Roelof van Ewijk and Cyrano Chatziantoniou are joint first author, both contributed equally to this work.

Alberto De Luca and Reineke A. Schoot are joint last author.

✉ Roelof van Ewijk
r.vanewijk-2@prinsesmaximacentrum.nl

Extended author information available on the last page of the article

Graphical Abstract



Keywords Biomarker · Diffusion magnetic resonance imaging · Rhabdomyosarcoma · Sarcoma · Surrogate marker

Introduction

Rhabdomyosarcoma is an aggressive soft tissue sarcoma. Currently, there is no reliable biomarker for use as a surrogate endpoint for long-term survival, with clear progression of the primary tumor and development of new lesions being the only features associated with a poorer outcome [1]. Earlier identification of poor or good responders to therapy may support the selection of patients eligible for treatment (de)intensification. Furthermore, it might support earlier evaluation of efficacy of strategies in international phase III studies, which now often require seven to ten years of patient recruitment and data accrual [2, 3].

Diffusion-weighted magnetic resonance imaging (DW-MRI), an imaging modality reflecting the average water displacement in tissues, has become a marker of interest for response assessment in oncology [4]. The apparent diffusion coefficient (ADC), derived from DW-MRI, is a quantification of the degree of free water motion. Tumors with high cellularity have a relative decrease in extracellular volume, which typically results in a decrease in ADC. Histological changes in the tumor, induced by chemotherapy for example, have been linked to changes in ADC, and as such, ADC has been investigated as a response marker in oncology [5, 6]. In pre-clinical rhabdomyosarcoma models, it has been shown that ADC might be reflective of Ki67 proliferation indices [7] and that therapy-induced tumor necrosis or growth corresponds with increases and decreases in ADC values, respectively [8]. However, the ADC data from current clinical studies [9–12] are insufficient for clinical implementation and do not adequately address factors potentially contributing to measurement variability, as reported in other tumor types [4].

In this study, we aimed to investigate the feasibility of DW-MRI in patients with rhabdomyosarcoma as a marker of response to neoadjuvant chemotherapy. As DW-MRI involves a number of technical choices and processing

steps, we evaluated the variability in DW-MRI acquisition protocols. An understanding of the variability, both technical and between patients, is essential to inform future prospective studies, because phase III studies in this rare tumor require the participation of over 100 hospitals. As such, the primary objectives of this retrospective study were to assess the degree of ADC change after chemotherapy; to describe the applied DW-MRI acquisition protocols; and to evaluate the impact of tumor segmentation variability on measured ADC values. Secondary objectives were to evaluate the association between ADC values and survival. The results of this feasibility study will be used to improve the methodology to accurately acquire, estimate and analyze DW-MRI markers in rhabdomyosarcoma.

Methods

Participant selection

Eligible patients were retrospectively selected from participating sites of the European *paediatric* Soft tissue sarcoma Study Group (EpSSG) RMS2005 and MTS2008 studies. The EpSSG RMS2005 and MTS2008 studies were approved by institutional review boards and all patients and/or parents gave written informed consent. Patients from The Netherlands, treated according to the EpSSG RMS2005 and MTS2008 protocols but not included in the study, signed informed consent as approved by the responsible authority. This retrospective study was approved by the medical research ethics committee (UMC Utrecht, reference-ID: 18–412).

Pediatric, adolescent and young adult patients, between 6 months and 21 years of age, with either localized or metastatic Intergroup Rhabdomyosarcoma Study (IRS) group III/IV histologically-proven rhabdomyosarcoma who were treated according to the EpSSG RMS2005 (ClinicalTrials.gov

identifier: NCT00379457) or *EpSSG* MTS2008 study (ClinicalTrials.gov identifier: NCT00379457) protocols with available DW-MRI scans were eligible. The *EpSSG* RMS2005 study was an academic, international, randomized, phase III trial, open from 2006 to 2016 including patients with localized rhabdomyosarcoma [2, 3]. The *EpSSG* MTS2008 study was an academic, international, prospective study, open from 2010 to 2016, including patients with metastatic rhabdomyosarcoma [13]. Survival was updated after closure of the studies. Participating centers were selected by the study national coordinators.

Imaging protocols

The study protocols included basic recommendations for MRI, without any specific guidance for DW-MRI sequences. All institutional MRI protocols were accepted. The baseline MRI was performed within 28 days of initiation of treatment. Early response evaluation per protocol was obtained after three 3-weekly cycles of chemotherapy. In case of protocol non-adherence, scans after two or four cycles with available DW-MRI were accepted.

Data collection and quality assessment

De-identified MRI data were collected on a platform developed as part of the Quality and Excellence in Radiotherapy and Imaging for Children and Adolescents with Cancer across Europe in Clinical Trials initiative of the European Society for Paediatric Oncology (SIOP Europe) [14]. MRI data were extracted and analyzed using an in-house program. Selected Digital Imaging and Communications in Medicine parameters essential for evaluation of DW-MRI technical variance (e.g., MRI vendor, TE, number of diffusion weightings (*B* values), maximum *B* value, echo time) were extracted. Intra-individual comparison of scan parameters between diagnosis and response was performed for heterogeneity; for continuous markers we considered parameters within a range of 10% between diagnosis and response as homogeneous. The diagnostic quality of each MRI was recorded by two pediatric radiologists (S.H. and R.R., with 10 and 18 years of experience in pediatric musculoskeletal radiology, respectively). A semi-quantitative scale, ranging from 1 to 3, was applied: 1 = poor, not evaluable (i.e. significant artefact); 2 = moderate, evaluable; 3 = good. Scans of poor quality were excluded from the analysis.

Tumor delineation

All scans were evaluated by one pediatric radiologist (S.H. or R.R.). Anatomical imaging (T1, T2, post-contrast T1) was reviewed and two-dimensional tumor segmentation on

a single axial DW-MRI slice was performed. A randomly selected subset of 20 patients were segmented by both radiologists for assessment of inter-observer variability, where the second delineation was performed on the same tumor slice. Investigators were blinded to patient characteristics and outcome. Single-slice segmentation was performed on the axial image with the largest proportion of homogeneous tumor. The inner edge of the tumor was delineated to minimize the risk of including peritumoral edema or adjacent tissues in the region-of-interest (ROI). Secondly, intralesional necrotic and cystic areas and artifacts were delineated (Fig. 1). For primary analysis, hemorrhage, cystic parts and artefacts were excluded.

Parameters

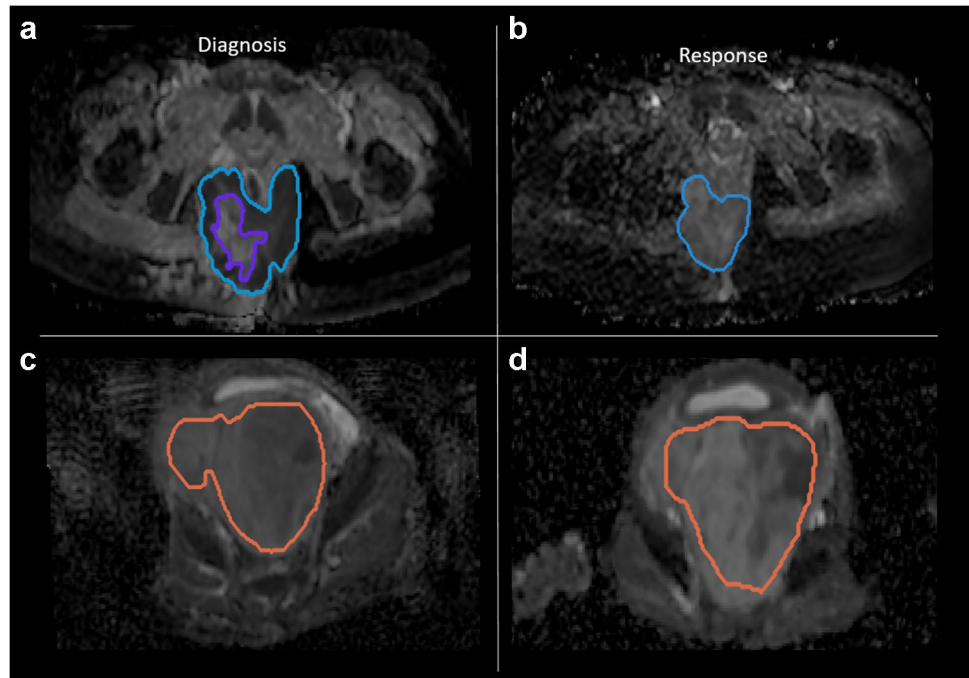
ADC was calculated from DW-MRI data where available. In the absence of raw DW-MRI data, ADC maps were used. The following ADC measures were extracted: mean, median, 5th percentile and 95th percentile. The choice for the 5th and 95th percentiles was made to reduce aberrant measures of minimal or maximum ADC due to artifacts. As such, we considered the 5th percentile an optimal measure of low ADC values.

Statistical analysis

The primary outcome of this study was the absolute change in mean ADC at the early response evaluation. ADC at diagnosis and early response were reported as secondary outcomes. ADC measures were compared between baseline and response using the paired *t*-test. The relation between stratifying patient and tumor characteristics (age, tumor size, *EpSSG* RMS2005 risk group [2, 3]) with ADC values at baseline or response was examined using the independent Student's *t*-test. For characteristics with more than two categories, an ANOVA was performed with Tukey's post hoc analysis. ADC measures were evaluated for the definition of the ROI and compared with paired *t*-test. We measured the inter-observer variability using the intraclass correlation coefficient for single measurements.

We evaluated the relation between ADC measures and event-free survival (EFS). An event was defined as disease progression, recurrence, or death due to any cause. A waterfall plot for the distribution of mean ADC change was used to visualize mean ADC change corresponding to the event status. Univariable Cox proportional hazard regression models were used to estimate the association between the ADC measures and EFS. For the analysis of mean ADC at baseline, the date of diagnosis was used. A landmark analysis at nine weeks after the date of diagnosis was used to estimate the association between change in mean ADC, mean ADC at response, and EFS [15, 16]. All statistical analyses were performed with R software version 4.1.1 [17].

Fig. 1 Tumor segmentation of diagnosis (**a, c**) and response (**b, d**) axial diffusion-weighted MRI (apparent diffusion coefficient) scans. **a, b** A 16-year-old girl with a perianal alveolar rhabdomyosarcoma. The whole tumor (blue outline) is delineated. The hemorrhagic component (inner purple outline in **a**) was excluded from the analysis. **c, d** A 1-year-old boy with a retroperitoneal pelvic rhabdomyosarcoma. The whole tumor (red outline) is delineated



Results

Patient characteristics

We enrolled 134 patients from seven countries (Belgium 10 patients; France 16; Italy 36; Norway 12; Spain 10; The Netherlands 46; UK 4). Median age was 6.0 years (range 0.3–21.8). Almost three-quarters of the patients had an embryonal rhabdomyosarcoma, nearly a quarter an alveolar rhabdomyosarcoma. Localized and metastatic disease were seen in 80% and 20% of patients, respectively (Table 1).

Diffusion-weighted magnetic resonance imaging quality assessment

In total, 268 scans were uploaded. After quality control, 199 scans were considered eligible. Reasons for exclusion were insufficient quality ($n=15$), no available DW-MRI scans ($n=20$), no measurable tumor ($n=33$) and tumor outside the field of view ($n=1$). The DW-MRI scans of 82 patients at diagnosis and at early response were included for analysis (Fig. 2).

Magnetic resonance imaging acquisition characteristics

Of 268 evaluated scans, 19 had no general scan characteristics available and 24 were without specific diffusion characteristics (Table 2). Intra-individual comparison of scans

showed that 14 patients had a different MRI manufacturer at diagnosis than at response (Supplementary Material 1). For the other selected parameters, comparison between diagnosis and response showed the average slice thickness to be more than 10% different in 26 patients; pixel spacing differed in 29 patients by more than 10%; and the mean echo time differed in 24 patients by more than 10%. In only 38 patients (46%) were technical parameters at diagnosis and at treatment response similar (Supplementary Material 2).

Apparent diffusion coefficient measurements

The mean ADC values were 1.1 (95% confidence interval [CI]: 1.1–1.2) at diagnosis and 1.6 (1.5–1.6) at response ($P<0.001$), for measurements excluding necrotic/cystic areas (Fig. 3). The mean absolute ADC change after neoadjuvant chemotherapy was 0.4 (0.3–0.5) and the mean percentage change was 44% (35–54). The mean of the median ADC was 1.1 (1.0–1.2) at diagnosis and 1.6 (1.5–1.7) at response ($P<0.001$). The median absolute ADC change was 0.5 (0.4–0.6) with an average median percentage change of 50% (39–61). The 5th percentile ADC was 0.8 (0.7–0.9) at diagnosis and 1.1 (1.0–1.2) at response ($P<0.001$). The 95th percentile ADC was 1.6 (1.5–1.6) at diagnosis and 2.0 (1.9–2.1) at response ($P<0.001$) (Table 3).

Apparent diffusion coefficient measurements, including necrotic/cystic regions

Mean ADC, including necrotic/cystic regions, was 1.1 (1.1–1.2) at diagnosis and 1.6 (1.5–1.6) at early response,

Table 1 Patient and tumor characteristics

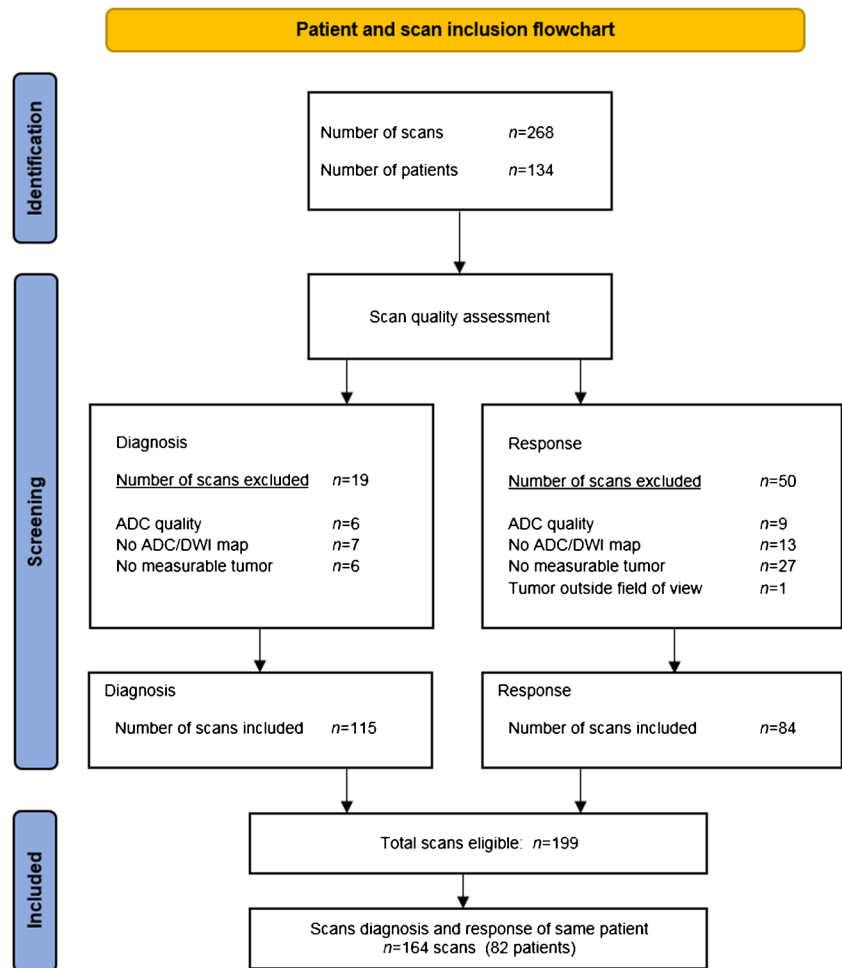
	Included patients (n=82)	Excluded patients (n=52)
Sex		
Female	22 (26.8%)	26 (50.0%)
Male	60 (73.2%)	26 (50.0%)
Age (years)		
Median [Min, Max]	5.9 [0.3, 21.8]	6.3 [0.6, 21.7]
Site of primary tumor		
Extremities	6 (7.3%)	6 (11.5%)
GUBP	18 (22.0%)	6 (11.5%)
GUnoBP	2 (2.4%)	1 (1.9%)
HNnoPM	10 (12.2%)	7 (13.5%)
HNPM	29 (35.4%)	18 (34.6%)
Orbit	9 (11.0%)	8 (15.4%)
Other site	8 (9.8%)	6 (11.5%)
Histology		
Alveolar	14 (17.1%)	15 (28.8%)
Embryonal	64 (78.0%)	32 (61.5%)
Other	4 (4.9%)	5 (9.6%)
Fusion status		
Negative	51 (62.2%)	27 (51.9%)
Positive	11 (13.4%)	10 (19.2%)
Missing	20 (24.4%)	15 (28.8%)
Tumor size		
≤ 5 cm	39 (47.6%)	31 (59.6%)
> 5 cm	43 (52.4%)	21 (40.4%)
Tumor stage		
T0	0 (0%)	1 (1.9%)
T1	31 (37.8%)	31 (59.6%)
T2	51 (62.2%)	20 (38.5%)
Nodal stage		
N0	58 (70.7%)	36 (69.2%)
N1	24 (29.3%)	16 (30.8%)
Risk group		
Standard	27 (32.9%)	20 (38.5%)
High	33 (40.2%)	18 (34.6%)
Very high	7 (8.5%)	2 (3.8%)
Metastatic	15 (18.3%)	12 (23.1%)

GUBP genitourinary bladder prostate, *GUnoBP* genitourinary non-bladder prostate, *HNPM* head neck par-
ameningeal, *HNnoPM* head neck non-parameningeal, *Max* maximum, *Min* minimum

which was not significantly different when compared to the mean ADC of ROI excluding these areas ($P=0.1$ and $P=0.42$, respectively). Absolute mean ADC change was 0.4 (0.3–0.5) and percentage ADC change was 44% (35–54), which was not significantly different to measurements excluding necrotic/cystic areas ($P=0.80$ and $P=0.81$, respectively), which was also observed in sub-analysis of patients with homogeneous scanning properties at diagnosis and response (Supplementary Material 3).

In subgroup analyses of all patients with necrotic/cystic areas delineated (nine at diagnosis and five at response), the mean ADC for scans including necrosis was on average 8% higher (range; 8% to 71%). Most scans, 12 out of 14, had a mean ADC difference variability within 10% when comparing ROIs with or without necrotic/cystic areas. There was one outlier, a diagnostic study of an embryonal rhabdomyosarcoma of the extremity with a large area of necrosis and a mean ADC of 2.3 versus 1.4 (excluding the necrotic region) (Fig. 4).

Fig. 2 Patient and scan selection. *ADC* apparent diffusion coefficient, *DWI* diffusion-weighted imaging



Apparent diffusion coefficient measurements for patient and tumor characteristics

In subgroup analysis of pediatric and adolescent patients up to 18 years of age (baseline characteristics in Supplementary Material 4 and 5), the mean ADC values of pediatric and adolescent patients were 1.1 (95% CI: 1.1–1.2) at diagnosis and 1.6 (1.5–1.6) at response. The mean absolute ADC change after neoadjuvant chemotherapy was 0.4 (0.3–0.5) and the mean percentage change was 45% (35–55). ADC values of the pediatric and adolescent patients were not significantly different as compared to the whole cohort (Supplementary Material 6). Direct comparison of ADC values of pediatric and adolescent patients ($n=81$) versus young adult patients ($n=1$) was not feasible.

For alveolar rhabdomyosarcoma ($n=14$), mean and median ADC at diagnosis were 1.0 (0.8–1.1) and 0.9 (0.7–1.1) versus 1.4 (1.3–1.6) and 1.4 (1.3–1.6) at response. For embryonal rhabdomyosarcoma ($n=64$), mean and median ADC at diagnosis, 1.2 (1.1–1.2) and 1.2 (1.1–1.2), respectively, were significantly higher compared to ADC in tumors with alveolar histology

($P=0.02$ and $P=0.01$). At response, mean and median of embryonal histology, 1.6 (1.5–1.7) and 1.6 (1.5–1.7), respectively, were not significantly different from alveolar histology ($P=0.11$ and $P=0.16$). Absolute change in mean ADC was 0.5 (0.2–0.7) for alveolar histology and 0.4 (0.3–0.5) for embryonal histology ($P=0.55$).

For tumors larger than 5 cm at diagnosis, mean and median ADC were 1.2 (1.1–1.2) and 1.1 (1.0–1.2), respectively at diagnosis versus 1.6 (1.5–1.7) and 1.6 (1.5–1.7), respectively at response. For tumors of 5 cm or smaller at diagnosis, mean and median ADC were 1.1 (1.0–1.2) and 1.1 (1.0–1.2), respectively at diagnosis versus 1.5 (1.4–1.7) and 1.6 (1.4–1.7), respectively at response. ADC measurements were not significantly different for tumor size at diagnosis.

ANOVA of mean and median ADC for treatment risk group showed a significant difference at diagnosis. No significant differences for risk group at response were identified. Tukey's post hoc test showed a significant difference in mean and median ADC at diagnosis between the very high–localized risk group versus the standard risk group ($P=0.03$ and $P=0.01$) and the high-risk group ($P=0.02$ and $P=0.01$). ADC mean and median in the very high–localized group at

Table 2 Diffusion-weighted magnetic resonance imaging acquisition characteristics

	Full cohort (n=268)
Manufacturer	
GE, Healthcare Technologies, Waukesha, WI, USA	23 (8.6%)
Philips, Best, The Netherlands	117 (43.7%)
Siemens, Erlangen, Germany	109 (40.7%)
Not available	19 (7.1%)
Slice thickness (mm)	
Mean (SD)	4.30 (0.975)
Median [Min, Max]	4.00 [2.00, 7.00]
Not available	19 (7.1%)
Number of B values	
Mean (SD)	2.93 (1.52)
Median [Min, Max]	2.00 [2.00, 10.0]
Not available	24 (9.0%)
Pixel spacing (mm)	
Mean (SD)	1.33 (0.448)
Median [Min, Max]	1.25 [0.332, 2.73]
Not available	19 (7.1%)
Highest B value	
Mean (SD)	962 (89.3)
Median [Min, Max]	1000 [800, 1400]
Not available	24 (9.0%)
Echo time (ms)	
Mean (SD)	78.0 (13.6)
Median [Min, Max]	77.8 [30.0, 134]
Not available	19 (7.1%)

Max maximum, Min minimum, SD standard deviation

diagnosis were 0.9 (0.8–0.9) and 0.8 (0.7–0.8), respectively. ADC mean and median were 1.2 (1.1–1.3) and 1.2 (1.1–1.3)

in the standard risk group, 1.2 (1.1–1.3) and 1.2 (1.0–1.3) in the high-risk group, and 1.1 (0.9–1.2) and 1.0 (0.9–1.1) in the very high–metastatic group, respectively (Table 3).

Apparent diffusion coefficient measurements for survival

The estimated hazard ratio from the univariable Cox hazard regression model showed no association at baseline between ADC 5th percentile (HR 95% CI: 0.2–2.6) or mean ADC (HR 95% CI: 0.1–1.6) and EFS. No association of ADC 5th percentile (HR 95% CI: 0.5–3.1) or mean ADC (HR 95% CI: 0.4–2.3) at response and absolute change in ADC 5th percentile (HR 95% CI: 0.61–3.9) or mean ADC (HR 95% CI: 0.6–3.2) and EFS was observed at the landmark point (Table 4, Fig. 5). Sub-analysis of the cohort with homogeneous scanning properties at diagnosis and response showed similar results (Supplementary Material 7).

Inter-observer variability

For inter-observer analysis, 20 patients were randomly selected. Intraclass correlation for mean ADC between two readers for selected slice delineation was 0.93 (95% CI: 0.83–0.97) for diagnosis and 0.96 (0.90–0.99) for response.

Discussion

This study shows a significant change in ADC 5th percentile, mean and median values of the primary tumor at response assessment after three cycles of chemotherapy. DW-MRI acquisition protocols showed high heterogeneity in and

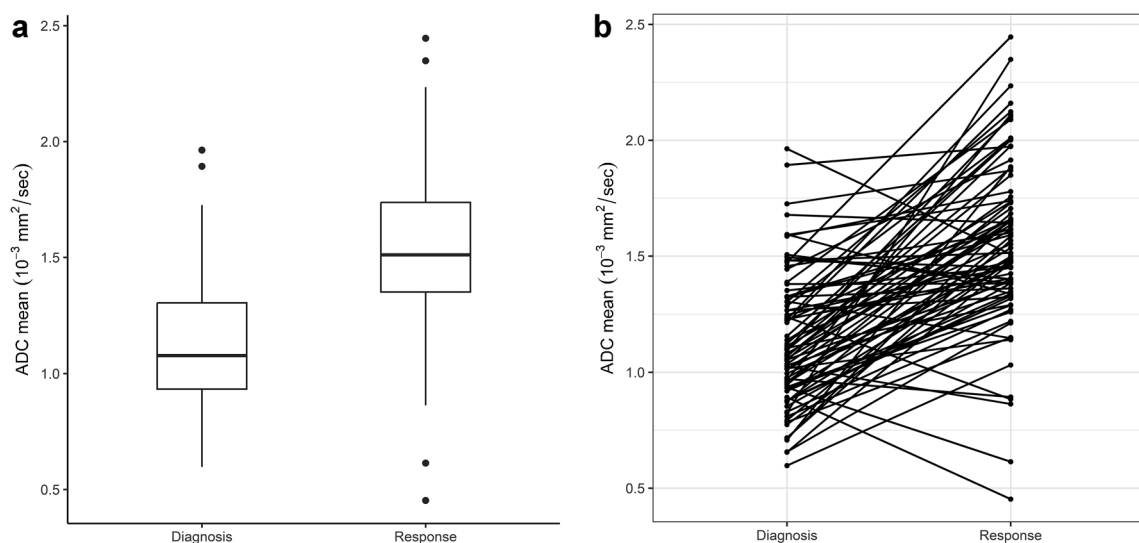


Fig. 3 Mean apparent diffusion coefficient (ADC) parameters excluding necrotic/cystic areas. **a** Boxplot shows values at diagnosis and response. **b** Graph shows individual changes in mean ADC at diagnosis and response

Table 3 Apparent diffusion coefficient values (95% confidence interval) based on tumor characteristics

ADC	Diagnosis	Response	Absolute change	Percentage change
Excluding necrotic/cystic areas				
Mean	1.13 (1.07–1.19)	1.55 (1.47–1.63)	0.42 (0.34–0.51)	44.2 (34.6–53.9)
Median	1.10 (1.04–1.17)	1.56 (1.48–1.65)	0.46 (0.37–0.56)	50.1 (39.1–61.2)
5th percentile	0.80 (0.74–0.86)	1.07 (0.98–1.15)	0.26 (0.18–0.34)	
95th percentile	1.55 (1.48–1.63)	2.01 (1.92–2.10)	0.46 (0.36–0.56)	
Including necrotic/cystic areas				
Mean	1.13 (1.07–1.19)	1.56 (1.48–1.64)	0.43 (0.34–0.51)	44.3 (34.6–54.0)
Median	1.10 (1.04–1.17)	1.57 (1.48–1.66)	0.47 (0.37–0.56)	50.4 (39.3–61.4)
5th percentile	0.80 (0.74–0.86)	1.06 (0.98–1.15)	0.26 (0.18–0.35)	
95th percentile	1.56 (1.48–1.64)	2.02 (1.93–2.11)	0.46 (0.36–0.56)	
Alveolar rhabdomyosarcoma				
Mean	0.96 (0.78–1.13)	1.42 (1.26–1.59)	0.46 (0.24–0.69)	55.4 (33.4–77.4)
Median	0.90 (0.73–1.07)	1.44 (1.25–1.62)	0.53 (0.30–0.77)	68.2 (40.5–95.9)
Embryonal rhabdomyosarcoma				
Mean	1.17 (1.11–1.24)	1.57 (1.48–1.67)	0.40 (0.30–0.50)	39.7 (28.6–50.9)
Median	1.16 (1.09–1.23)	1.58 (1.48–1.68)	0.42 (0.31–0.53)	43.5 (31.1–55.8)
Tumor size ≤ 5 cm				
Mean	1.11 (1.02–1.20)	1.54 (1.41–1.68)		
Median	1.10 (1.01–1.19)	1.56 (1.42–1.70)		
Tumor size > 5 cm				
Mean	1.15 (1.05–1.24)	1.56 (1.47–1.66)		
Median	1.11 (1.01–1.20)	1.57 (1.46–1.67)		
Standard risk group				
Mean	1.17 (1.06–1.28)	1.51 (1.33–1.69)		
Median	1.17 (1.05–1.28)	1.53 (1.34–1.72)		
High-risk group				
Mean	1.19 (1.07–1.30)	1.60 (1.51–1.70)		
Median	1.16 (1.04–1.28)	1.62 (1.51–1.72)		
Very high–localized				
Mean	0.85 (0.78–0.91)	1.65 (1.26–2.04)		
Median	0.77 (0.70–0.84)	1.69 (1.24–2.13)		
Very high–metastatic				
Mean	1.05 (0.94–1.16)	1.47 (1.28–1.66)		
Median	1.01 (0.91–1.12)	1.46 (1.26–1.66)		

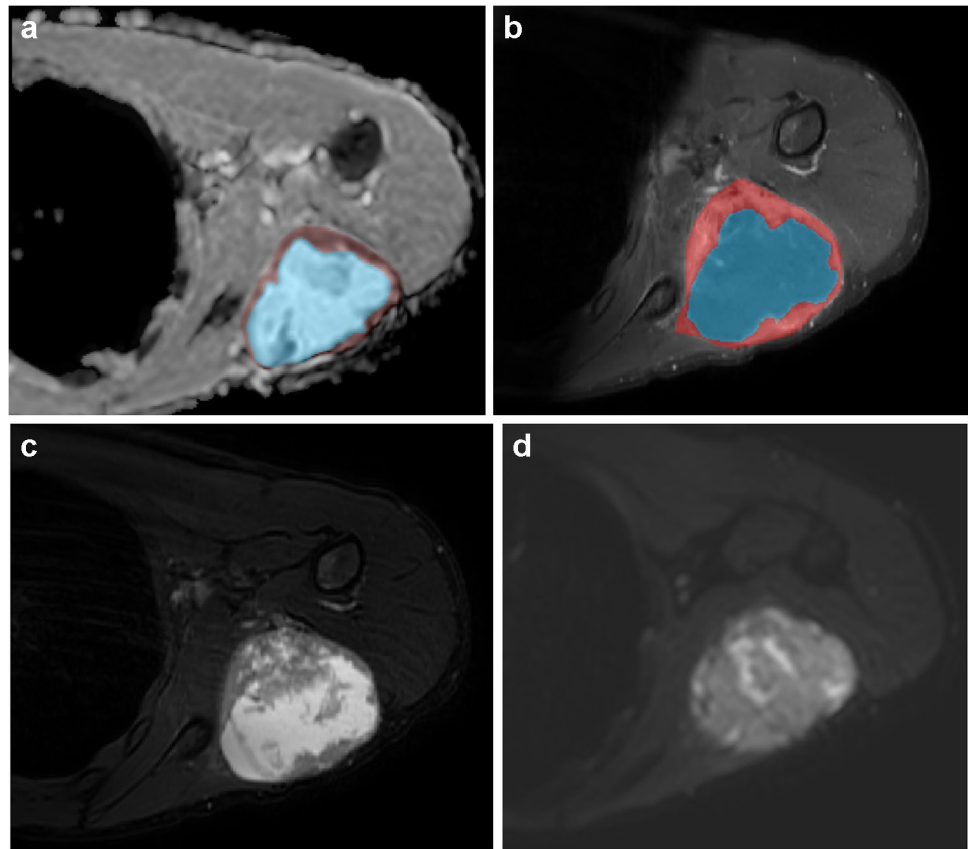
ADC apparent diffusion coefficient

among individuals when comparing scans at diagnosis and response. Exploratory analyses of mean ADC revealed a significant difference for tumor histology and risk group status at baseline. Univariable Cox regression analysis did not show an association between the change in the ADC 5th percentile or mean ADC and EFS. Analysis of inter-observer variability in a selected group exhibited excellent agreement.

The change in ADC after chemotherapy identified in this study is in line with preclinical research [7]. However, whereas in other solid cancers, like brain [18] and breast tumors [19, 20], DW-MRI has become standard in diagnostic and response imaging, studies in rhabdomyosarcoma are thus far mainly focused on diffusion measurements at presentation to narrow

the differential diagnosis of a soft tissue mass [5, 21]. Available reports have mainly focused on patients with head-neck rhabdomyosarcoma [9]. As such, comparative studies for this work in rhabdomyosarcoma, as for soft tissue sarcoma, are limited. The prognostic value of baseline ADC and diffusion restrictive volume in children and adolescents with head-neck rhabdomyosarcoma has been described in one retrospective cohort [11]. Although the included cohort differed in tumor location and age compared to this study, the mean reported ADC of 1.04 [11] is in a similar range to our observation of mean ADC at diagnosis. The authors concluded that lower ADC at baseline might correlate with overall survival, which in our view might be explained by alveolar histology of six patients in the study,

Fig. 4 A 14-year-old boy with an embryonal rhabdomyosarcoma of the left upper extremity, located in the teres minor, with central necrosis. Axial apparent diffusion coefficient (ADC) (a), T1 post-contrast (b), T2 (c) and diffusion-weighted (d) images. The mean ADC was 71% higher when including compared to excluding the necrotic region. Blue intra-tumoral hemorrhage, brown/red tumor tissue



given that in our study we observed lower mean and median ADC values for patients with alveolar compared to embryonal rhabdomyosarcoma. However, it is unclear what the underlying biological explanation is. The question of whether low mean ADC at diagnosis is an independent risk factor needs to be investigated including in the analysis known risk factors such as histology and fusion status, for localized and metastatic rhabdomyosarcoma [13, 22–24].

In our study, we describe the heterogeneity of DW-MRI acquisition parameters, as it is reported to be an important source of variability for quantitative applications. In the literature, the underlying tumor biology, the scan operator,

the hardware and software of the MRI system, including the DW-MRI acquisition protocol, the algorithm to convert DW-MRI to ADC and definition of ROIs are considered to be the most important factors leading to variability [4]. In our study, DW-MRI systems and acquisition protocols were frequently different within individuals, explained in several ways. First, frequently an MRI is performed before referral to a tertiary center and is not always repeated. Second, due to the rarity of the disease, scan operators might not be familiar with soft tissue sarcoma-specific protocols. This is complicated by the fact that rhabdomyosarcoma may occur anywhere in the body, and thus different scanning protocols, specific for body sites, are in

Fig. 5 Waterfall plot showing mean apparent diffusion coefficient (ADC) percentage change per patient for patients with and without a tumor-related event

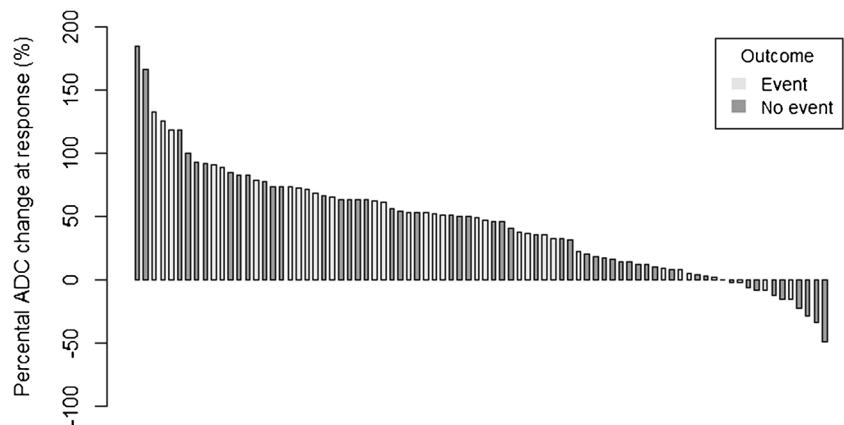


Table 4 Univariable Cox proportional hazard analysis for event-free survival

Variable		Hazard ratio	(95% CI)
ADC 5th percentile	Absolute change	1.5	(0.61–3.9)
Mean ADC	Absolute change	1.3	(0.57–3.2)
ADC 5th percentile	Diagnosis	0.72	(0.2–2.6)
Mean ADC	Diagnosis	0.43	(0.11–1.6)
ADC 5th percentile	Response	1.3	(0.52–3.1)
Mean ADC	Response	0.92	(0.37–2.3)

ADC apparent diffusion coefficient, CI confidence interval

practice. Lastly, we observed that the raw DW-MRI data were not always stored, which limited our ability to recalculate the ADC independent of the system software. As only 46% of the included cohort of our study had similar DW-MRI parameters, technical variability is an important subject in this and for future studies in this tumor.

We evaluated the difference between two different ROIs. In the literature, a wide methodological variety in the definition of ROIs is described in sarcoma [25]. A proof-of-concept study showed higher ADC measurements when including necrotic or cystic areas [25]. Although we did not observe a significant difference in ADC values, on an individual level, potentially relevant differences were identified when validating ADC as an individual response marker to therapy. Investigating the measurement variability caused by technical factors is an interesting topic for further research.

In our study, we present a cohort of rhabdomyosarcoma patients who underwent DW-MRI. Multiple limitations are important to acknowledge. In 20% of the eligible patients, early response assessment after three cycles was not possible due to the lack of measurable tumor. This complicates the clinical validation and implementation of DW-MRI as a response marker, as patients with complete remission (non-measurable disease) at early response evaluation were not reported to be a prognostic subgroup [1, 26]. Furthermore, due to lack of MRI standardization, high heterogeneity was observed in this retrospective study, which limits the validity of our results.

To improve quantitative DW-MRI studies, we will need to evaluate the magnitude of the impact of technical variability on ADC measurements. It will be essential to investigate methods for optimal procedures in data acquisition and quality control and assurance for harmonization and standardization of DW-MRI data to be representative and of diagnostic quality, as, for example, performed in quantitative fluorodeoxyglucose-positron emission tomography imaging by the European Association of Nuclear Medicine [1, 27, 28]. To raise awareness and improve protocol adherence, a European rhabdomyosarcoma imaging guideline was developed in a multi-organizational collaboration, including technical MRI protocols [29]. For validation and trial design of quantified imaging biomarkers, the Quantitative

Imaging Biomarkers Alliance of the Radiological Society of North America and the European Imaging Biomarker Alliance of the European Society of Radiology provide guidance for methodological standards [30–32], which will be incorporated in the upcoming prospective study.

In conclusion, we have demonstrated the feasibility of ADC measurement in rhabdomyosarcoma and highlight important methodological considerations to take forward in prospective assessments of the predictive value of DW-MRI as a response marker.

Supplementary Information Supplementary material is available at <https://doi.org/10.1007/s00247-023-05745-z>.

Acknowledgements The authors would like to thank all patients and parents for contributing.

The authors would like to thank Sarah Kelly and Anne Blondeel within of the Quality and Excellence in Radiotherapy and Imaging for Children and Adolescents with Cancer across Europe in Clinical Trials (QUARTET) group of the European Society of Paediatric Oncology (SIOPE), Hafida Lmalem imaging manager of the European Organisation for Research and Treatment of Cancer (EORTC) and Nicola Fenwick of the Cancer Research UK Clinical Trials Unit (CRCTU) for their support in the design of the data collection platform and logistics.

The authors would like to thank Ilaria Zanetti and Beatrice Copadoro of the clinical trials unit of the Pediatric Hematology Oncology Division, University Hospital of Padua, and the Department of Women's and Children's Health, University of Padua, Padua, Italy, for their help with the extraction of the retrospective RMS2005 and MTS2008 data of the European paediatric Soft tissue sarcoma Study Group (EpSSG).

Author contribution Conceptualization: R.E., C.C., S.H., A.L., J.M., R.R., A.L., R.S. Methodology: R.E., C.C., M.F., S.H., A.L., J.M., R.R., A.D.L., R.S. Formal analysis and investigation: R.E., C.C., R.D., M.F., S.H., R.R. Writing — original draft preparation: R.E., C.C. Writing — review and editing: M.A., P.B., G.B., A.B., P.C.D., V.C., A.C., R.D., C.D., G.D., A.F., M.F., S.G., C.G., H.G., S.H., M.J., W.K., A.L., J.L., H.M., K.M., J.M., V.M., S.M., C.M., D.O., L.O.M., E.P., P.D.P., K.P., L.Q., M.R., R.R., A.R., S.S., A.D.L., R.S. Funding acquisition: S.H., A.L., J.M., R.R., A.D.L., R.S. Resources: M.A., P.B., G.B., A.B., P.C.D., V.C., A.C., C.D., G.D., A.F., S.G., C.G., H.G., M.J., W.K., J.L., H.M., K.M., V.M.C., S.M., C.M., D.O., L.O.M., E.P., P.D.P., K.P., L.Q., M.R., A.R., S.S. Supervision: A.L., J.M., R.R., A.D.L., R.S. All authors reviewed and approved the final manuscript.

Funding R.E. and C.C. are funded by the KIKA Foundation (Children Cancer-free, number 357). H.M. acknowledges NHS funding from the NIHR Biomedical Research Centre at The Royal Marsden and The Institute of Cancer Research.

Data Availability The datasets generated during and/or analyzed during the current study are available from the corresponding author on reasonable request.

Declarations

Conflicts of interest None

Open Access This article is licensed under a Creative Commons Attribution 4.0 International License, which permits use, sharing, adaptation, distribution and reproduction in any medium or format, as long as you give appropriate credit to the original author(s) and the source,

provide a link to the Creative Commons licence, and indicate if changes were made. The images or other third party material in this article are included in the article's Creative Commons licence, unless indicated otherwise in a credit line to the material. If material is not included in the article's Creative Commons licence and your intended use is not permitted by statutory regulation or exceeds the permitted use, you will need to obtain permission directly from the copyright holder. To view a copy of this licence, visit <http://creativecommons.org/licenses/by/4.0/>.

References

- van Ewijk R, Vaarwerk B, Breunis WB, Schoot RA, Ter Horst SAJ, van Rijn RR, van der Lee JH, Merks JHM (2021) The value of early tumor size response to chemotherapy in pediatric rhabdomyosarcoma. *Cancers (Basel)* 13(3):510
- Bisogno G, Jenney M, Bergeron C, GallegoMelcon S, Ferrari A, Oberlin O, Carli M, Stevens M, Kelsey A, De Paoli A, Gaze MN, Martelli H, Devalck C, Merks JH, Ben-Arush M, Glosli H, Chisholm J, Orbach D, Minard-Colin V, De Salvo GL, European paediatric Soft tissue sarcoma Study G (2018) Addition of dose-intensified doxorubicin to standard chemotherapy for rhabdomyosarcoma (EpSSG RMS 2005): a multicentre, open-label, randomised controlled, phase 3 trial. *Lancet Oncol* 19:1061–1071
- Bisogno G, De Salvo GL, Bergeron C, GallegoMelcon S, Merks JH, Kelsey A, Martelli H, Minard-Colin V, Orbach D, Glosli H, Chisholm J, Casanova M, Zanetti I, Devalck C, Ben-Arush M, Mudry P, Ferman S, Jenney M, Ferrari A, European paediatric Soft tissue sarcoma Study G (2019) Vinorelbine and continuous low-dose cyclophosphamide as maintenance chemotherapy in patients with high-risk rhabdomyosarcoma (RMS 2005): a multicentre, open-label, randomised, phase 3 trial. *Lancet Oncol* 20:1566–1575
- Taouli B, Beer AJ, Chenevert T, Collins D, Lehman C, Matos C, Padhani AR, Rosenkrantz AB, Shukla-Dave A, Sigmund E, Tanenbaum L, Thoeny H, Thomassin-Naggara I, Barbieri S, Corcuera-Solano I, Orton M, Partridge SC, Koh DM (2016) Diffusion-weighted imaging outside the brain: Consensus statement from an ISMRM-sponsored workshop. *J Magn Reson Imaging* 44:521–540
- Humphries PD, Sebire NJ, Siegel MJ, Olsen OE (2007) Tumors in pediatric patients at diffusion-weighted MR imaging: apparent diffusion coefficient and tumor cellularity. *Radiology* 245:848–854
- Donati F, Boraschi P, Pacciardi F, Cervelli R, Castagna M, Urbani L, Falaschi F, Caramella D (2017) 3T diffusion-weighted MRI in the response assessment of colorectal liver metastases after chemotherapy: Correlation between ADC value and histological tumour regression grading. *Eur J Radiol* 91:57–65
- Yuan Y, Zeng D, Zhang Y, Tao J, Liu Y, Lkhagvadorj T, Yin Z, Wang S (2020) Intravoxel incoherent motion diffusion-weighted imaging assessment of microvascular characteristics in the murine embryonal rhabdomyosarcoma model. *Acta Radiol* 61:260–266
- Thoeny HC, De Keyzer F, Vandecaveye V, Chen F, Sun X, Bosmans H, Hermans R, Verbeken EK, Boesch C, Marchal G, Landuyt W, Ni Y (2005) Effect of vascular targeting agent in rat tumor model: dynamic contrast-enhanced versus diffusion-weighted MR imaging. *Radiology* 237:492–499
- Norman G, Fayer D, Lewis-Light K, McHugh K, Levine D, Phillips B (2015) Mind the gap: extent of use of diffusion-weighted MRI in children with rhabdomyosarcoma. *Pediatr Radiol* 45:778–781
- Soldatos T, Ahlawat S, Montgomery E, Chalian M, Jacobs MA, Fayad LM (2016) Multiparametric Assessment of Treatment Response in High-Grade Soft-Tissue Sarcomas with Anatomic and Functional MR Imaging Sequences. *Radiology* 278:831–840
- Pourmehdi Lahiji A, Jackson T, Nejadnik H, von Eyben R, Rubin D, Spunt SL, Quon A, Daldrup-Link H (2019) Association of Tumor [(18)F]FDG Activity and Diffusion Restriction with Clinical Outcomes of Rhabdomyosarcomas. *Mol Imaging Biol* 21:591–598
- Theruvath AJ, Siedek F, Muehe AM, Garcia-Diaz J, Kirchner J, Martin O, Link MP, Spunt S, Pribnow A, Rosenberg J, Herrmann K, Gatidis S, Schafer JF, Moseley M, Umutlu L, Daldrup-Link HE (2020) Therapy Response Assessment of Pediatric Tumors with Whole-Body Diffusion-weighted MRI and FDG PET/MRI. *Radiology* 296:143–151
- Schoot RA, Chisholm JC, Casanova M, Minard-Colin V, Geoerger B, Cameron AL, Coppadoro B, Zanetti I, Orbach D, Kelsey A, Rogers T, Guizani C, Elze M, Ben-Arush M, McHugh K, van Rijn RR, Ferman S, Gallego S, Ferrari A, Jenney M, Bisogno G, Merks JHM (2022) Metastatic Rhabdomyosarcoma: Results of the European Paediatric Soft Tissue Sarcoma Study Group MTS 2008 Study and Pooled Analysis With the Concurrent BERNIE Study. *J Clin Oncol* 40(32):3730–3740
- Kelly SM, Effenev R, Gaze MN, Bernier-Chastagner V, Blondeel A, Clementel E, Corning C, Dieckmann K, Essiaf S, Gandola L, Janssens GO, Kearns PR, Lacombe D, Lassen-Ramshad Y, Merks H, Miles E, Padovani L, Scarzello G, Schwarz R, Timmermann B, van Rijn RR, Vassal G, Boterberg T, Mandeville HC, Project Q, the SROWG (2022) QUARTET: A SIOP Europe project for quality and excellence in radiotherapy and imaging for children and adolescents with cancer. *Eur J Cancer* 172:209–220
- Buyse M, Piedbois P (1996) On the relationship between response to treatment and survival time. *Stat Med* 15:2797–2812
- Anderson JR, Cain KC, Gelber RD (1983) Analysis of survival by tumor response. *J Clin Oncol* 1:710–719
- (2022) R Core Team. R: A language and environment for statistical computing. R Foundation for Statistical Computing, Vienna, Austria URL <https://www.R-project.org/>
- Erker C, Tamrazi B, Poussaint TY, Mueller S, Mata-Mbemba D, Franceschi E, Brandes AA, Rao A, Haworth KB, Wen PY, Goldman S, Vezina G, MacDonald TJ, Dunkel IJ, Morgan PS, Jaspas T, Prados MD, Warren KE (2020) Response assessment in paediatric high-grade glioma: recommendations from the Response Assessment in Pediatric Neuro-Oncology (RAPNO) working group. *Lancet Oncol* 21:e317–e329
- Lo Gullo R, Sevilimedu V, Baltzer P, Le Bihan D, Camps-Herrero J, Clauser P, Gilbert FJ, Iima M, Mann RM, Partridge SC, Patterson A, Sigmund EE, Thakur S, Thibault FE, Martincich L, Pinker K, group EIBD-WIw (2022) A survey by the European Society of Breast Imaging on the implementation of breast diffusion-weighted imaging in clinical practice. *Eur Radiol* 32:6588–6597
- Baltzer P, Mann RM, Iima M, Sigmund EE, Clauser P, Gilbert FJ, Martincich L, Partridge SC, Patterson A, Pinker K, Thibault F, Camps-Herrero J, Le Bihan D, group EIBD-WIw, (2020) Diffusion-weighted imaging of the breast—a consensus and mission statement from the EUSOBI International Breast Diffusion-Weighted Imaging working group. *Eur Radiol* 30:1436–1450
- Kocaoglu M, Bulakbasi N, Sanal HT, Kismet E, Caliskan B, Akgun V, Tayfun C (2010) Pediatric abdominal masses: diagnostic accuracy of diffusion weighted MRI. *Magn Reson Imaging* 28:629–636
- Hibbitts E, Chi YY, Hawkins DS, Barr FG, Bradley JA, Dasgupta R, Meyer WH, Rodeberg DA, Rudzinski ER, Spunt SL, Skapek SX, Wolden SL, Arndt CAS (2019) Refinement of risk stratification for childhood rhabdomyosarcoma using FOXO1 fusion status in addition to established clinical outcome predictors: A report from the Children's Oncology Group. *Cancer Med* 8:6437–6448
- Haduong JH, Heske CM, Allen-Rhoades W, Xue W, Teot LA, Rodeberg DA, Donaldson SS, Weiss A, Hawkins DS, Venkatramani R (2022) An update on rhabdomyosarcoma risk stratification and the rationale for current and future Children's Oncology Group clinical trials. *Pediatr Blood Cancer* 69:e29511
- Gallego S, Zanetti I, Orbach D, Ranchere D, Shipley J, Zin A, Bergeron C, de Salvo GL, Chisholm J, Ferrari A, Jenney M, Mandeville HC, Rogers T, Merks JHM, Mudry P, Glosli H, Milano GM, Ferman S, Bisogno G, European Paediatric Soft Tissue

- Sarcoma Study G (2018) Fusion status in patients with lymph node-positive (N1) alveolar rhabdomyosarcoma is a powerful predictor of prognosis: Experience of the European Paediatric Soft Tissue Sarcoma Study Group (EpSSG). *Cancer* 124:3201–3209
25. Chatziantoniou C, Schoot RA, van Ewijk R, van Rijn RR, Ter Horst SAJ, Merks JHM, Leemans A, De Luca A (2023) Methodological considerations on segmenting rhabdomyosarcoma with diffusion-weighted imaging-What can we do better? *Insights Imaging* 14:19
 26. Rosenberg AR, Anderson JR, Lyden E, Rodeberg DA, Wolden SL, Kao SC, Parham DM, Arndt C, Hawkins DS (2014) Early response as assessed by anatomic imaging does not predict failure-free survival among patients with Group III rhabdomyosarcoma: a report from the Children's Oncology Group. *Eur J Cancer* 50:816–823
 27. Boellaard R, Delgado-Bolton R, Oyen WJ, Giammarile F, Tatsch K, Eschner W, Verzijlbergen FJ, Barrington SF, Pike LC, Weber WA, Stroobants S, Delbeke D, Donohoe KJ, Holbrook S, Graham MM, Testanera G, Hoekstra OS, Zijlstra J, Visser E, Hoekstra CJ, Pruim J, Willemsen A, Arends B, Kotzerke J, Bockisch A, Beyer T, Chiti A, Krause BJ, European Association of Nuclear M (2015) FDG PET/CT: EANM procedure guidelines for tumour imaging: version 2.0. *Eur J Nucl Med Mol Imaging* 42:328–354
 28. Vali R, Alessio A, Balza R, Borgwardt L, Bar-Sever Z, Czachowski M, Jehanno N, Kurch L, Pandit-Taskar N, Parisi M, Piccardo A, Seghers V, Shulkin BL, Zucchetto P, Lim R (2021) SNMMI Procedure Standard/EANM Practice Guideline on Pediatric (18) F-FDG PET/CT for Oncology 1.0. *J Nucl Med* 62:99–110
 29. van Ewijk R, Schoot RA, Sparber-Sauer M, Ter Horst SAJ, Jehanno N, Borgwardt L, de Keizer B, Merks JHM, de Luca A, McHugh K, von Kalle T, Schafer JF, van Rijn RR, Cooperative WeichteilsarkomStudiengruppe Imaging Group tESoPROTF, the European Paediatric Soft Tissue Sarcoma Study Group Imaging C (2021) European guideline for imaging in paediatric and adolescent rhabdomyosarcoma - joint statement by the European Paediatric Soft Tissue Sarcoma Study Group, the Cooperative Weichteilsarkom Studiengruppe and the Oncology Task Force of the European Society of Paediatric Radiology. *Pediatr Radiol* 51:1940–1951
 30. Raunig DL, McShane LM, Pennello G, Gatsonis C, Carson PL, Voyvodic JT, Wahl RL, Kurland BF, Schwarz AJ, Gonen M, Zahlmann G, Kondratovich MV, O'Donnell K, Petrick N, Cole PE, Garra B, Sullivan DC, Group QTPW (2015) Quantitative imaging biomarkers: a review of statistical methods for technical performance assessment. *Stat Methods Med Res* 24:27–67
 31. Sullivan DC, Obuchowski NA, Kessler LG, Raunig DL, Gatsonis C, Huang EP, Kondratovich M, McShane LM, Reeves AP, Barboriak DP, Guimaraes AR, Wahl RL, Group R-QMW (2015) Metrology Standards for Quantitative Imaging Biomarkers. *Radiology* 277:813–825
 32. deSouza NM, van der Lugt A, Deroose CM, Alberich-Bayarri A, Bidaut L, Fournier L, Costaridou L, Oprea-Lager DE, Kotter E, Smits M, Mayerhoefer ME, Boellaard R, Caroli A, de Geus-Oei LF, Kunz WG, Oei EH, Lecouvet F, Franca M, Loewe C, Lopei E, Caramella C, Persson A, Golay X, Dewey M, O'Connor JPB, deGraaf P, Gatidis S, Zahlmann G, European Society of R, European Organisation for R, Treatment of C (2022) Standardised lesion segmentation for imaging biomarker quantitation: a consensus recommendation from ESR and EORTC. *Insights Imaging* 13:159

Publisher's note Springer Nature remains neutral with regard to jurisdictional claims in published maps and institutional affiliations.

Authors and Affiliations

Roelof van Ewijk¹ · Cyrano Chatziantoniou^{1,2} · Madeleine Adams³ · Patrizia Bertolini⁴ · Gianni Bisogno^{5,6} · Amine Bouhamama⁷ · Pablo Caro-Dominguez⁸ · Valerie Charon⁹ · Ana Coma¹⁰ · Rana Dandis¹ · Christine Devalck¹¹ · Giulia De Donno² · Andrea Ferrari¹² · Marta Fiocco^{1,13} · Soledad Gallego¹⁴ · Chiara Giraudo¹⁵ · Heidi Glosli¹⁶ · Simone A. J. ter Horst¹⁷ · Meriel Jenney¹⁸ · Willemijn M. Klein¹⁹ · Alexander Leemans² · Julie Leseur²⁰ · Henry C. Mandeville²¹ · Kieran McHugh²² · Johannes H. M. Merks^{1,23} · Veronique Minard-Colin²⁴ · Salma Moalla²⁵ · Carlo Morosi²⁶ · Daniel Orbach²⁷ · Lil-Sofie Ording Muller²⁸ · Erika Pace²⁹ · Pier Luigi Di Paolo³⁰ · Katia Perruccio³¹ · Lucia Quaglietta³² · Marleen Renard³³ · Rick R. van Rijn³⁴ · Antonio Ruggiero³⁵ · Sara I. Sirvent³⁶ · Alberto De Luca^{2,37} · Reineke A. Schoot¹

¹ Princess Máxima Center for Pediatric Oncology, Heidelberglaan 25, 3584 CS Utrecht, The Netherlands

² Image Sciences Institute, UMC Utrecht, Utrecht, The Netherlands

³ Department of Paediatric Oncology, Children's Hospital for Wales, University Hospital, Cardiff, UK

⁴ Pediatric Hematology-Oncology Unit University-Hospital of Parma, Parma, Italy

⁵ Department of Women's and Children's Health, University of Padua, Padua, Italy

⁶ Pediatric Hematology Oncology Division, University Hospital of Padua, Padua, Italy

⁷ Service de Radiologie Interventionnelle Oncologique, Centre Léon Bérard, Lyon, France

⁸ Pediatric Radiology Unit, Department of Radiology, Hospital Universitario Virgen del Rocío, Avenida Manuel Siurot S/N, Seville, Spain

⁹ Radiology Department, CHU Rennes, Rennes, France

¹⁰ Paediatric Radiology Unit, Vall d'Hebron Hospital Campus, Barcelona, Spain

¹¹ Department of Hemato-Oncology, HUB, ULB, HUDERF, Brussels, Belgium

¹² Pediatric Oncology Unit, Fondazione IRCCS Istituto Nazionale Tumori, Milan, Italy

¹³ Mathematical Institute, Leiden University, Leiden, The Netherlands

¹⁴ Pediatric Oncology Department, Vall d'Hebron Hospital, Barcelona, Spain

¹⁵ Unit of Advanced Clinical and Translational Imaging, Department of Medicine-DIMED, University of Padova, 35122 Padua, Italy

¹⁶ Department of Paediatric Research, Division of Paediatric and Adolescent Medicine, Oslo University Hospital, Oslo, Norway

¹⁷ Department of Radiology and Nuclear Medicine, Wilhelmina Children's Hospital, UMC Utrecht, Utrecht, The Netherlands

¹⁸ Paediatric Oncology, Cardiff and Vale UHB, Cardiff, UK

¹⁹ Department of Medical Imaging, Radboud University Medical Center, Nijmegen, the Netherlands

²⁰ Service de Radiothérapie, Centre Eugène Marquis, Rennes, France

²¹ Department of Radiotherapy, The Royal Marsden Hospital and The Institute of Cancer Research, Sutton, UK

²² Department of Radiology, Great Ormond Street Hospital for Children, NHS Foundation Trust, London, UK

²³ Division of Imaging and Oncology, University Medical Center Utrecht, Utrecht University, Utrecht, The Netherlands

²⁴ Department of Pediatric and Adolescent Oncology, Gustave Roussy Cancer Campus, Université Paris-Saclay, Villejuif, France

²⁵ Department of Imaging, Institut Gustave Roussy, Villejuif, France

²⁶ Diagnostic and Interventional Radiology, Fondazione IRCCS Istituto Nazionale Dei Tumori, Milan, Italy

²⁷ SIREDO Oncology Center (Care, Innovation and Research for Children and AYA With Cancer), Institut Curie, PSL Research University, Paris, France

²⁸ Department of Radiology and Intervention Unit for Paediatric Radiology, Oslo University Hospital, Ullevål, Norway

²⁹ Department of Radiology, The Royal Marsden NHS Foundation Trust, London, UK

³⁰ Department of Radiology, Bambino Gesù Children's Hospital, IRCCS, Rome, Italy

³¹ Pediatric Hematology Oncology, Azienda Ospedaliera Universitaria, Ospedale Santa Maria Della Misericordia, Perugia, Italy

³² Neuro-Oncology Unit, Department of Paediatric Oncology, Santobono-Pausilipon Children's Hospital, Naples, Italy

³³ Department of Paediatric Hemato-Oncology, University Hospital Leuven, Louvain, Belgium

³⁴ Department of Radiology and Nuclear Medicine, Amsterdam UMC Location University of Amsterdam, Amsterdam, the Netherlands

³⁵ Pediatric Oncology Unit, Fondazione Policlinico Universitario A. Gemelli IRCCS, Università Cattolica del Sacro Cuore, Rome, Italy

³⁶ Pediatric Radiology Department, Hospital Niño Jesús, Madrid, Spain

³⁷ Department of Neurology, UMC Utrecht Brain Center, UMC Utrecht, Utrecht, The Netherlands